Anal. Bioanal. Electrochem., Vol. 13, No. 2, 2021, 264-282

Analytical & Bioanalytical Electrochemistry

2021 by CEE
www.abechem.com

Full Paper

A Sensitive Method for the Electrochemical Determination of Tramadol, Codeine and Caffeine by A CeO_2-SnO_2/rGO Nanocomposite-Modified Glassy Carbon Electrode

Farzad Hosseini, Manochehr Bahmaei,* and Mehran Davallo

Department of Chemistry, Islamic Azad University, North Tehran Branch, Tehran, Iran

*Corresponding Author, Tel.: +982163962417

E-Mail: m_bahmaei@iau-tnb.ac.ir

Received: 27 April 2021 / Received in revised form: 10 September 2021 / Accepted: 15 September 2021 / Published online: 30 September 2021

Abstract- The CeO_2-SnO_2/rGO was synthesized and used for modification of glassy carbon electrode (GCE) to measurement of Tramadol (Tra), Codeine (Cod) and Caffeine (Caf). Electrical impedance spectroscopy (EIS) techniques showed that CeO_2-SnO_2/rGO/GCE has the lower electron transfer resistance (R_{ct}) (63 Ω) in comparison to GCE (223 Ω) and was suitable for electrochemical applications. The synthesized nanomaterials were investigated by some methods such as Transmission electron microscopy (TEM), X-ray Diffraction (XRD), and Fourier-transform infrared spectroscopy (FTIR). The pH value was investigated in the range of 5.5 to 9.5 which the best signal was obtained at pH=6.5. At the CeO_2-SnO_2/rGO/GCE three oxidation peaks appeared at 0.755, 1.05, and 1.412 V with Ip_a= 22.1, 78.4 and 69.49 µA for Tra, Cod, and Caf and the peaks separation of ΔEp (Tra-Cod)= 295 mV, and ΔEp (Cod-Caf)=362 mV in the potential region 0.4-1.6 V. In optimum condition, a dynamic range of 0.008-10 µM and 10-270 µM for Tra, 0.01-12 µM and 12-260 µM for Cod, 0.01-14 µM and 14-260 µM for Caf with the detection limit of 0.0056, 0.0053, and 0.0055 µM for of Tra, Cod and Caf, respectively, were obtained. Investigation of effect of scan rate (25 and 300 mV/s) shows that the electrode process was diffusion-controlled. Interference studies show that Li^+, Na^+, K^+, Cl^-, Ca^{2+}, Uric acid, Ascorbic acid, Morphine, sucrose, and glucose have no effect on the oxidation current of the analytes. Finally, the presented electrochemical electrode was applied for the measurement of Tra, Cod and Caf in urine and human plasma spiked samples.

Keywords- Tramadol; Codeine; Caffeine; Glassy carbon electrode; Reduced graphene oxide; Metal oxide nanoparticle

1. INTRODUCTION

Tra or (1R,2R)-2-[(dimethylamino)methyl]-1-(3-methoxyphenyl) cyclohexanol is one of the popular painkillers and opioid analgesic which has an agonist impact on the μ-opioid receptor in the human body. The high efficacy of Tra for the management of moderate to intense pain associated with no clinically striking effects on respiratory or cardiovascular parameters, dissimilar other opioids, and lower potential for producing abuse or dependence led to the appearance of several pharmaceutical dosage forms in the market [1].

Cod or 3-methylmorphine is an opiate that can be extracted from the poppy plant or synthesized in the laboratory, used for its analgesic, antitussive, and antidiarrheal properties for pharmaceutical use. Also, it could be used to treat diarrhea. Cod could be attached to specific proteins throughout the brain and body to alleviate pain. similar many drugs, using the Cod or the high dose of it could cause side effects in some patients. Some of its side effects are constipation, feeling sleepy and confused, dry mouth, seizures, and muscle stiffness [2].

Caf or 3,7-dihydro-1,3,7-trimethyl-1H purine-2,6-dione or 1,3,7- trimethyl xanthine is a natural alkaloid stimulant to the central nervous system, and every year about 120,000 tons of it has been used worldwide. Caf generally used in energy drinks, food supplements, and drugs. Although the Caf improves consciousness and athletic strength, it causes metabolism acceleration and diuresis, bronchial muscle relaxation, blood pressure promotion, central nervous system stimulation. High levels of Caf in the human body cause disorders that can include: heart diseases, kidney failure, vomiting, and trembling [3]. Therefore, when used to reduce pain, they can be present in body fluids simultaneously. Also, these analytes are used simultaneously in some drugs. On the other hand, these compounds are taken as model compounds to demonstrate the performances and usefulness of the sensor for applications in the pharmaceutical field.

Nowadays, providing an accurate and reproducible method that can measure drugs in biological fluids in a short time is one of the most critical challenges for analytical chemists [4-9].

So, the scientists attempt to present a rapid and simple method with high selectivity and reliable data to determine of ions, drugs, and biomolecules [4,10-13]. There are several methods for this aim, such as electrochemical methods, high-performance liquid chromatography, spectrophotometry, gas chromatography–mass spectrometry, liquid chromatography–mass spectrometry, chemiluminescence, capillary electrophoresis–mass, and spectrometry [4]. Electrochemical methods have their advantages due to their simplicity, inexpensive instrument, and speed [5-16], so it was used for create new, simple and sensitive method for determination drugs in complex matrix.

To our knowledge in the literature, there are a lot of researches about the individual electrochemical determination of drugs such as Tra, Cod and, Caf. Still, there is no research that determines the Tra, Cod and, Caf, simultaneously. Owing to exceptional mechanical and

chemical stability, electrical conductivity, surface area, one effective way to improve the signal-to-noise ratio in electrochemical methods is using nanoparticles or nanocomposites for modification of electrodes.

Recently, metal and metal oxide NPs has been receiving great attention mainly in the field of electrochemical sensor and biosensors due to their high potential and versatility to become very competitive materials for modifying the morphology, chemical stability and physicochemical interfacial properties of conventional sensing materials. The processes involved in sensing with metal oxide NPs sensors are extremely complex. In fact, metal oxide NPs can be assembled to form tandem heterostructures, hybrid structures or composite structures with advanced electrochemical properties which can be adapted for a specific sensor application. These materials could be changed the number of transferred electrons or changes in mass or redox potential for various analytes on electrochemical sensors. Also, Parameters like sensitivity, selectivity, response time and stability of sensors can be further improved by the addition of different dopants, which act to change the activation energy, to generate oxygen vacancy or to change the electronic structure/band gap. Also, the reduced graphene oxide can improve the conductivity and the electrochemical surface area of the electrodes. In the other hand, doping of two or three metal oxide NPs in the matrix of nanocomposite can boost the conductivity of the electrochemical sensor. In this research, we tried to use two metal oxides as well as carbon-based nanomaterials and investigate the synergistic effect.

The reduced graphene oxide (rGO) [17], CeO_2 [18], and SnO_2 nanoparticles [19] owning to their potential can apply in different sensors, batteries, transistors, and using as catalysts [20]. The combination of these three nanoparticles can be favorable for improving the electrochemical properties.

In the presented study, the CeO_2-SnO_2/rGO was synthesized and applied for surface correction of GCE. The CeO_2-SnO_2/rGO nanocomposite was investigated by TEM, XRD, and FTIR. EIS was used for investigation the electrochemical efficiency of CeO_2-SnO_2/rGO/GCE. Under optimum condition, CeO_2-SnO_2/rGO/GCE illustrates high activity for electrooxidation of Tra, Cod, and Caf; also, the presented sensor was successfully applied for measurement of the Tra, Cod, and Caf in some real samples.

2. EXPERIMENTAL

2.1. Chemicals and apparatus

The chemicals for the preparation of CeO_2-SnO_2/rGO nanocomposite, include Graphite powder with <20 μm diameter (purity >99.9), cerium (III) nitrate hexahydrate (purity 99% trace metals basis), Tin (II) chloride dehydrate (purity 98%), ammonium hydroxide (28% NH3 in H_2O), Triethanolamine (purity ≥99.0%), isopropyl alcohol (purity≥99.7%), benzoquinone (purity≥98%), sulfuric acid (95.0-98.0%), hydrogen peroxide (30 % (w/w) in H_2O),

hydrochloric acid (37%), potassium permanganate (≥99.0%), NaOH (≥98%) and Tramadol hydrochloride (≥98%), Caf (≥98%) and Cod (≥98%) were purchase from Merck Company and consumed without further refinement. Deionized water was used to prepare all aqueous solutions. pH adjustment of solution was done using Britton-Robinson universal buffer solution (B-R buffer solution), also it was used as supporting electrolytes.

All optimization tests and determination processes were performed at the laboratory temperature by Autolab electrochemical system (Model PGSTAT 302 N potentiostat/ galvanostat, EcoChemie, The Netherlands). Three-electrode include Ag/AgCl/KCl (3 M) electrode as a reference electrode, modified and unmodified GCE as working electrode and Pt wire as the counter electrode were used for voltammetric investigations. The electrochemical impedance spectra and voltammograms were analyzed using the Nova 1.7 software. The Metrohm pH meter (model 713-Switzerland) was applied for Checking the pH. TEM image was taken using Zeiss EM902A (Germany). FTIR spectra were obtained by a Perkin-Elmer spectrophotometer (Spectrum GX), and XRD patterns were determined by an XRD (38066 Riva, d/G.Via M. Misone, 11/D (TN) Italy) at ambient temperature.

2.2. Synthesis of the modifiers and construction of working electrodes

Graphene oxide (GO) were synthesized from graphite powder using improved Hummer-Offeman's method. In the first step, 160 ml sulfuric acid was added to 40 ml orthophosphoric acid, after mixing the solution 1.6 g graphite powder was added (mixed for 1 h). After that, 9 g potassium permanganate was added to the mixture (mixed for 72 h at 25 ºC). Then, hydrogen peroxide solution (30% in H_2O) was added dropwise to the prepared suspension until turns into yellow color. The new suspension was centrifuged and washed with 1 M HCl solution, deionized water/ethanol three times. The obtained GO was dried in a vacuum at 80 ºC for 12 h [21].

In the next step, the rGO was prepared by reduction of GO by hydrazine hydrate. A 1 mg/ml suspension of GO was prepared in 150 ml H_2O. Then 2 ml hydrazine hydrate was added to the suspension and kept at 100 ºC for 24 h. The obtained rGO was centrifuged, washed with deionized water three times, and finally dried in a vacuum at 80 ºC for 12 h [21].

The SnO_2/rGO nanocomposite was prepared by hydrothermal treatment of $SnCl_2$ H_2O solutions in the presence of synthesized rGO. In the first step, suspension of rGO in water was prepared by dispersing 100 mg rGO in 60 mL DDW and sonicating for 1 h. 0.26 g $SnCl_2$ H_2O was added to the suspension and sonicated for 35 min. The obtained mixture was transferred to a 100 mL Teflon-lined stainless-steel autoclave then heated at 185 °C for 30 h. Afterward, obtained nanocomposite was centrifuged (3000 rpm for 20 min) and in order to remove chloride ion washed 3 times by DDW/ethanol (50/50 v/v) [22].

The CeO_2-SnO_2/rGO nanocomposite was provided by the hydrothermal treatment. 200 mg prepared SnO_2/rGO and 500 mg $Ce(NO_3)_3.6H_2O$ was added to 60 mL DDW, and stirring for

45 min. Then, the obtained suspension was transferred to a 100 mL Teflon-lined stainless-steel autoclave then heated at 160 °C for 20 h. The produced was collected and washed 3 times by DDW/ethanol (50/50 v/v) [22].

The bare GCE (activated GCE) was provided by polishing its surface with alumina powder with 0.05 mm to a mirror-like surface. Also, to prepare the surface of GCE for the placement of modifiers, it was immersed in diluted nitric acid and HCl and finally washed with DDW 3 times [23]. The modified GCEs include rGO/GCE, SnO_2/rGO/GCE, and CeO_2-SnO_2/rGO/GCE were constructed by dropping 10 µl suspension (1 mg/ml) of rGO, SnO_2/rGO, and CeO_2-SnO_2/rGO nanocomposite in DMF onto the surface of the bare GCEs, then it was dried at ambient temperature [23].

Graphene oxide (GO) were synthesized from graphite powder using improved Hummer-Offeman's method. In the first step, 160 ml sulfuric acid was added to 40 ml orthophosphoric acid, after mixing the solution 1.6 g graphite powder was added (mixed for 1 h). After that, 9 g potassium permanganate was added to the mixture (mixed for 72 h at 25 ^oC). Then, hydrogen peroxide solution (30% in H_2O) was added dropwise to the prepared suspension until turns into yellow color. The new suspension was centrifuged and washed with 1 M HCl solution, deionized water/ethanol three times. The obtained GO was dried in a vacuum at 80 ^oC for 12 h [21].

In the next step, the rGO was prepared by reduction of GO by hydrazine hydrate. A 1 mg/ml suspension of GO was prepared in 150 ml H_2O. Then 2 ml hydrazine hydrate was added to the suspension and kept at 100 ^oC for 24 h. The obtained rGO was centrifuged, washed with deionized water three times, and finally dried in a vacuum at 80 ^oC for 12 h [21].

The SnO_2/rGO nanocomposite was prepared by hydrothermal treatment of $SnCl_2$ H_2O solutions in the presence of synthesized rGO. In the first step, suspension of rGO in water was prepared by dispersing 100 mg rGO in 60 mL DDW and sonicating for 1 h. 0.26 g $SnCl_2$ H_2O was added to the suspension and sonicated for 35 min. The obtained mixture was transferred to a 100 mL Teflon-lined stainless-steel autoclave then heated at 185 °C for 30 h. Afterward, obtained nanocomposite was centrifuged (3000 rpm for 20 min) and in order to remove chloride ion washed 3 times by DDW/ethanol (50/50 v/v) [22].

The CeO_2-SnO_2/rGO nanocomposite was provided by the hydrothermal treatment. 200 mg prepared SnO_2/rGO and 500 mg $Ce(NO_3)_3.6H_2O$ was added to 60 mL DDW, and stirring for 45 min. Then, the obtained suspension was transferred to a 100 mL Teflon-lined stainless-steel autoclave then heated at 160 °C for 20 h. The produced was collected and washed 3 times by DDW/ethanol (50/50 v/v) [22].

The bare GCE (activated GCE) was provided by polishing its surface with alumina powder with 0.05 mm to a mirror-like surface. Also, to prepare the surface of GCE for the placement of modifiers, it was immersed in diluted nitric acid and HCl and finally washed with DDW 3 times [23]. The modified GCEs include rGO/GCE, SnO_2/rGO/GCE, and CeO_2-

SnO_2/rGO/GCE were constructed by dropping 10 µl suspension (1 mg/ml) of rGO, SnO_2/rGO, and CeO_2-SnO_2/rGO nanocomposite in DMF onto the surface of the bare GCEs, then it was dried at ambient temperature [23].

2.3. Preparation of real sample and spiked sample

The capability of the CeO_2-SnO_2/rGO/GCE for measurement of Tra, Cod, and Caf in Human serum and urine samples was examined. The Human serum and urine samples were collected from a non-smoking volunteer (male, 36 years, 100 kg, and 179 cm). The 10 and 20 µM of each analyte were added to the collected samples, and the determination process was repeated in order to the calculation of recovery percentages. The urine sample was placed in a refrigerator after their collection. 20 mL of the collected sample was centrifuged for 20 min at 3000 rpm. The supernatant was filtered (0.45 mm filter) and diluted 5 times with B-R buffer solution (pH = 6.5). The collected serum sample was centrifuged (20 min at 3000 rpm) and filtering by a 0.45 mm filter, then it was diluted with B-R buffer solution (pH =6.5) [23].

3. RESULTS AND DISCUSSION

3.1. Structural investigation of the nanocomposite

The XRD analysis are shown in Fig. 1a. The related XRD patterns of GO and rGO represent typical characteristic peaks at 2θ=10.81° (001) and 25.78° (002), respectively, which is consistent with previous studies. So, the results confirm that GO is converted to rGO by $NaBH_4$. The diffraction peaks of the SnO_2/rGO represents the peaks at 26.49°, 33.16°, 37.50°, and 51.53° can be assigned to (110), (101), (211) and (112) planes, respectively, are ascribed to the tetragonal structure and are well agree with JCPDS no. 41-1445 [24]. Also, it can be seen that, no prominent diffraction peaks corresponding to rGO are observed in the XRD pattern of the SnO_2/rGO nanocomposite. The XRD pattern of CeO_2-SnO_2/rGO ternary nanocomposite displays eight separate peaks at 2θ= 28.73°, 33.33°,47.58°, and 56.39° which are related to the cubic fluorite-type structure of CeO_2 nanoparticles (JCPDS no. 34-0394) and 26.77°, 30.07°, 37.77°, and 51.80° (are related to SnO_2 nanoparticles) [22]. The XRD data confirm the successful synthesis of GO, rGO, SnO_2/rGO, and CeO_2-SnO_2/rGO nanomaterials.

The FT-IR spectral analysis was applied to the investigate of surface functional groups and the interaction between the components in CeO_2-SnO_2/rGO ternary nanocomposite (Fig. 1b). The FTIR spectrum of GO nanosheet represents six main peaks at 3235 (O−H stretching), 2842 (C−H stretching), 1720 (C=O stretching), 1616 (C-O-H vibration), 1354 (C−O stretching), and 1271 (C=C stretching) cm^{-1} [25]. By using $NaBH_4$ as a reduction agent, the FTIR peak intensity of oxide groups in GO has reduced, which corroborant the synthesis of rGO [25]. In the FTIR spectrum of SnO_2/rGO nanocomposite, the peaks at 819 cm^{-1} (was related to O-Sn-O stretching vibration) and 534 cm^{-1} (was appointed to the Sn-O stretching vibration) [22]. In the FTIR

spectrum of CeO_2-SnO_2/rGO ternary nanocomposite, in addition to peaks related to tin oxide, the peaks below 750 cm^{-1} were attributed to the Ce-O-Ce stretching vibration. The broad FTIR peak in 3382 cm^{-1} can be indexed to adsorbed water-bound molecules and O−H stretching vibration [22]. The observed peaks in the ternary nanocomposite confirmed the successful incorporation of CeO_2, and SnO_2 nanoparticles into the rGO nanosheets.

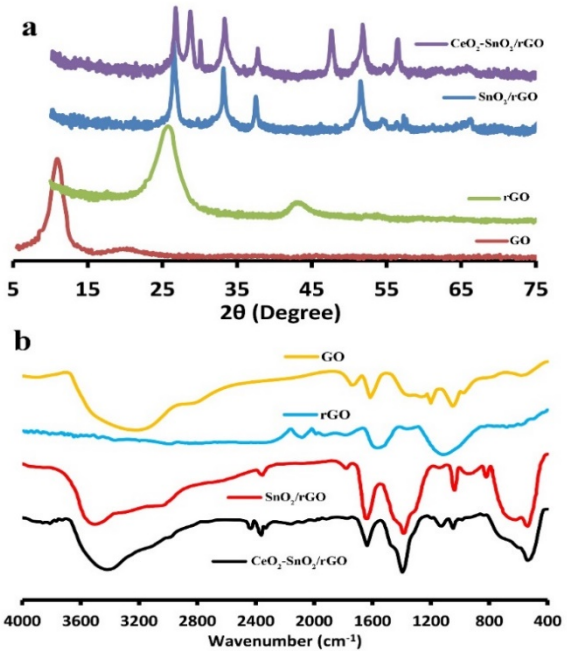

Fig. 1. a) XRD pattern and b) FTIR spectrum of GO, rGO, SnO_2/rGO and CeO_2-SnO_2/rGO

For more study, the surface morphology, size, and dispersion of nanoparticles in the prepared CeO_2-SnO_2/rGO ternary nanocomposite were investigated by TEM. The obtained TEM image is provided in Fig. 2a.

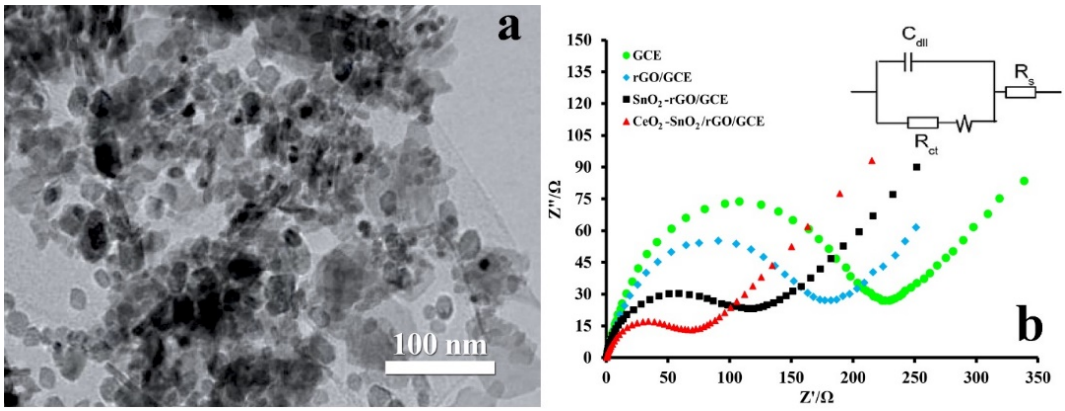

Fig. 2. a) TEM image of CeO_2-SnO_2/rGO and b) Characterization of GCE, rGO/GCE, SnO_2-rGO/GCE, and CeO_2-SnO_2/rGO/GCE by EIS

The image clearly shows that CeO_2 and SnO_2 were uniformly distributed on the surface of rGO with a smaller size than that of rGO. This kind of nanometer size of particles can act as a site of electrochemical reaction sites.

3.2. Electrochemical impedance spectroscopy study

The surface property of the different using GCEs was investigated in the presence of 5.0 mM $[Fe(CN)_6]^{3-/4-}$ and 1.0 M KCl by and EIS in the frequency range of 100 kHz to 0.1 Hz. The diameter of the semicircle of the Nyquist plot represents electron transfer resistance (R_{ct}) of the GCEs that were changed by the different electrodes. It can be said when the resistance decreased, the mobility of electrons on the surface of the electrode has increased subsequently. Fig. 2b depicts the characteristic Nyquist plot of GCE, rGO/GCE, SnO_2/rGO/GCE, and CeO_2-SnO_2/rGO/GCE by R_{ct} value of 223, 173, 100, and 63, respectively.

A semicircle with the largest diameter was observed for the GCE; however, the diameter of the semicircle had decreased when the rGO was employed for modification of GCE. On using SnO_2-rGO/GCE, the semicircle domain was severely smaller than GCE, and rGO/GCE. The presence of SnO_2/rGO nanocomposite accelerated the electron transfer process, so that it can enhance the sensitivity of the constructed sensor toward the analytes. It can be seen that there is a smaller semicircle for CeO_2-SnO_2/rGO/GCE, denoting that there is the best electron mobility in this electrode in comparison to the other using electrodes. Hence CeO_2-SnO_2/rGO ternary nanocomposite in the surface of GCE boost the electron transfer between the $[Fe(CN)6]^{3-/4-}$ complex and the electrode surface owing to the larger surface area and better conductivity of the nanomaterials. Therefore, CeO_2-SnO_2/rGO/GCE is the best candidate among the others investigated electrodes for applying in electrochemical measurement of some analytes.

3.3. Electrochemical oxidation studies of Tra, Cod and Caf at the surface of different electrodes

The electrochemical behavior of 40 μM Tra, Cod and Caf in B-R buffer solution pH=6.5 at the surface of GCE, rGO/GCE, SnO_2/rGO/GCE and CeO_2-SnO_2/rGO/GCE were investigated by differential pulse voltammetry (DPV) techniques, and the voltammograms are represented in Fig. 3a.

At bare GCE, there was capacitive current with two low current electrochemical signals for Cod, and Caf in 1.16 and 1.5 V, respectively. There is no peak for Tra at the surface of GCE. This treatment of the analytes at the surface of the GCE suggests that the electrooxidation behavior was sluggish. The rGO/GCE represents responses for Cod, and Caf with the larger current than GCE; also a weak peak for Tra was observed in the voltammogram at 0.78 V. Three sharp oxidation peaks appeared at 0.755, 1.05, and 1.412 V with Ip_a= 15.2, 55.3 and 45.5 μA for Tra, Cod, and Caf at the surface of SnO_2-rGO/GCE, it can be seen that the peaks

separation ΔEp (Tra-Cod)=295 mV, and ΔEp (Cod-Caf)=362 mV, so simultaneous measurement of these three analytes can be done. The modified GCE with CeO_2-SnO_2/rGO nanocomposite represents three sharp, and well-defined peaks for Tra, Cod, and Caf at the same potential were those of SnO_2-rGO/GCE. The peaks currents for Tra, Cod, and Caf at CeO_2-SnO_2/rGO/GCE were 22.1, 78.4 and 69.49 µA, which were 1.45, 1.42, and 1.53 times larger than the Ip_a at SnO_2-rGO/GCE, which make CeO_2-SnO_2/rGO/GCE the best choice for concurrent determination of Tra, Cod, and Caf with the lowest detection limit (DL) and high sensitivity. In the absence of Tra, Cod, and Caf and in B-R buffer solution pH=6.5, the CeO_2-SnO_2/rGO/GCE did not show any observable oxidation peak in the potential region 0.4-1.6 V. For this reason, CeO_2-SnO_2/rGO/GCE was selected as the optimal electrode for subsequent experiments.

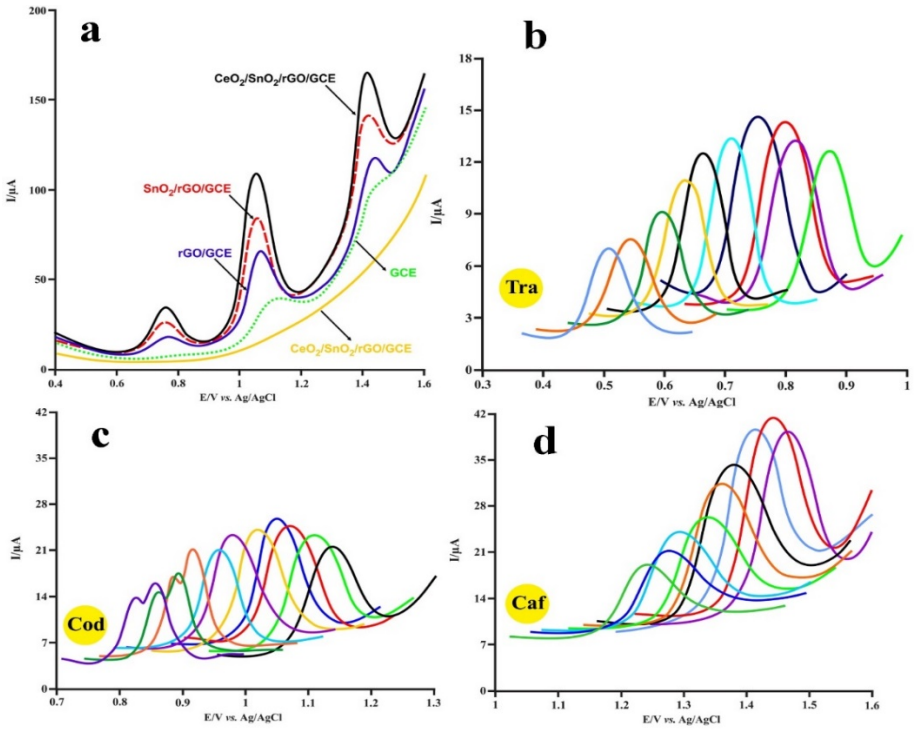

Fig. 3. a) Electrochemical oxidation of Tra, Cod and Caf at GCE, rGO/GCE, SnO_2-rGO/GCE and CeO_2-SnO_2/rGO/GCE, and Effect of pH on electrooxidation of b) Tra, c) Cod, d) Caf

3.4. Effect of pH on electrooxidation of Tra, Cod, and Caf

The amount of hydrogen ion in the solution can affect the electrooxidation properties, include the potential, and current of the drugs peak. Therefore, the electrochemical behavior of 8 µM Tra, 5 µM Cod, and 7 µM Caf was studied at various pH values between 5.5 to 9.5 at the surface of CeO_2-SnO_2/rGO/GCE using DPV in 0.2 M B–R buffer solutions. The voltammograms are presented in Fig. 3b-d.

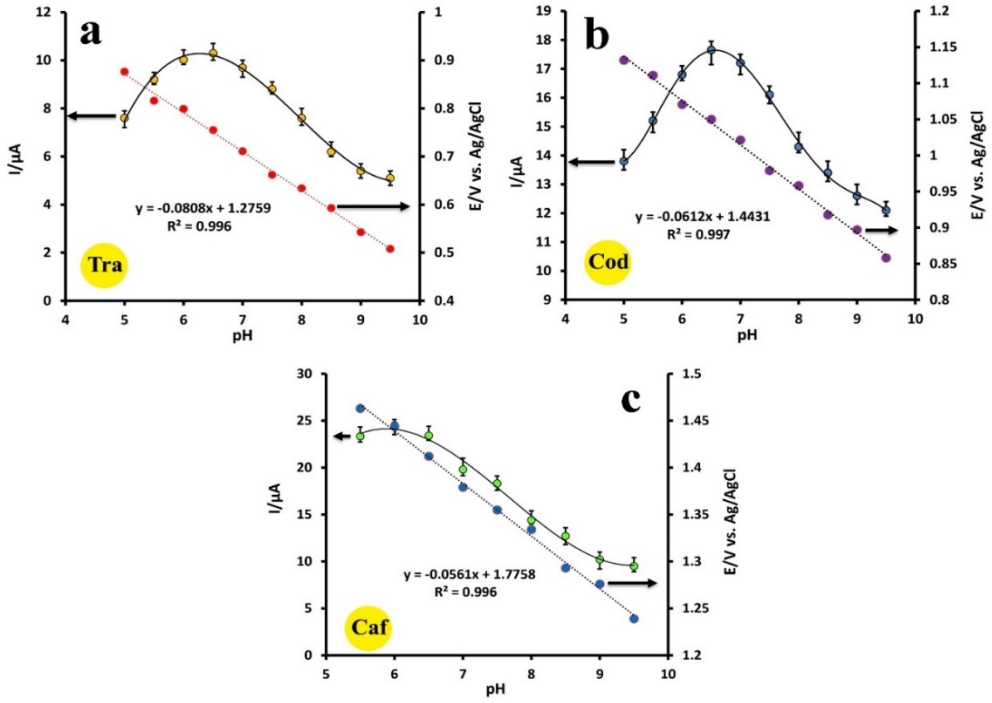

Fig. 4. Plot of I *vs.* pH and E *vs.* pH for a) Tra, b) Cod and c) Caf

The data shows that the peak current of Tra and Cod has increased while the pH value have changed from 5.5 to 6.5. Then, as the pH increases between 6.5 and 9.5, the peak current of oxidation of Tra, and Cod have decreased gradually. On the electrochemical oxidation of Caf, the maximum peak current obtained in pH=5.5, and with increasing the pH value from 6 to 9.5, the electrochemical response has decreased significantly. Also, no oxidation peak was observed for Tra in pH 2 to 5.

The results demonstrate that the oxidation peak potentials of Tra, Cod, and Caf have shifted to less potential values while the pH values have changed from 5.5 to 9.5, suggesting that hydrogen ion participates in the electrooxidation process. The plots of the Ep vs. pH are shown in Fig. 4 a-c, and the relationship could be described by the following equations:

Tra	Ep = -0.0808 pH + 1.2759	$R^2 = 0.996$	Eq. 1
Cod	Ep = -0.0612 pH + 1.4431	$R^2 = 0.997$	Eq. 2
Caf	Ep = -0.0561 pH + 1.7758	$R^2 = 0.996$	Eq. 3

The slope of obtained equations is close to the Nernstian slop value (0.059 V/pH at 25 ºC), the result indicate that the number of hydrogen ions and electrons is equal.

The slope of the equation related to Cod and Caf showed a value of -0.0612 and -0.0561 mV/pH, respectively, which are close to the Nernstian slope value. The change in potential

displays that the ratio of the number of electrons/protons which involved in the electro-oxidation of Cod, and Caf is about 1, on the surface of CeO_2-SnO_2/rGO/GCE.

For Cod, in the pH range of 5.5 to 8, an anodic peak appeared, and base on previous reports, it could be the result of the sum of two close peaks. The observed peak may be related to the electrooxidation of the tertiary amine and the 6-hydroxy groups of Cod, which are almost superimposed [26,27].

At pH 8.5, 9, and 9.5, the voltammograms showed a new small peak beside the main peak of Cod. The appearance of two oxidation peaks should result from oxidation of the mentioned groups, which are now separated.

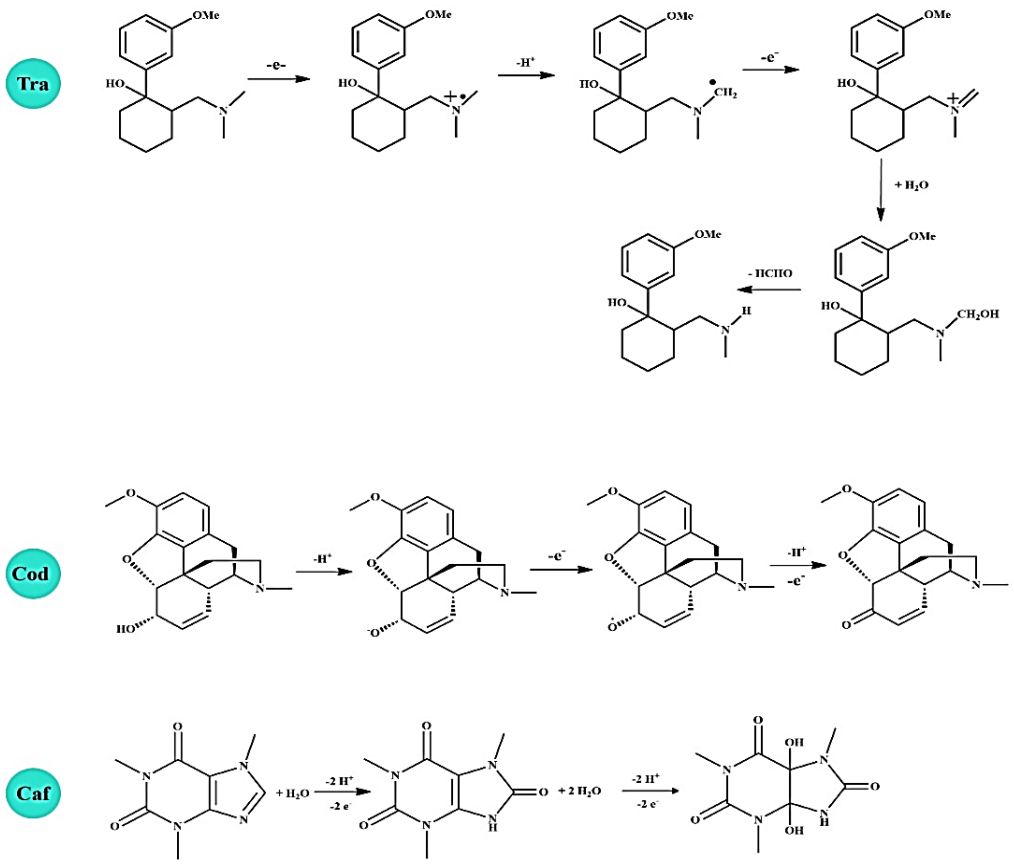

Scheme 1. Proposed electrooxidation mechanism of Tra, Cod and Caf at the surface of CeO_2-SnO_2/rGO/GCE

3.5. The impact of scan rate and instrumental parameters on the electro-oxidation of Tra, Cod and Caf

The influence of varying scan rate on the oxidation currents of CeO_2-SnO_2/rGO/GCE for electrooxidation of 8 µM Tra, 5 µM Cod and Caf was investigated by CV technique. The

obtained CVs for the three analytes at different scan rates from 25 to 300 mV/s are represented in Fig. 5a.

The CVs for the three analytes showed irreversible processes that the oxidation currents were growth by incrementing the sweep rate. Moreover, the potential of oxidation peaks has shifted to positive direction. The oxidation peak currents changed in a linear relationship with the square root of scan rates for three analytes. The linear regression equations for Tra, Cod and Caf were found as Ip = 0.7315 $v^{1/2}$ - 1.1919 (R^2 = 0.993), Ip = 1.1721 $v^{1/2}$ - 1.4916 (R^2 = 0.998) and Ip = 1.0069 $v^{1/2}$ - 0.9619 (R^2 = 0.996), respectively (Fig. 4b). The obtained results demonstrate that the electrochemical reactions of Tra, Cod, and Caf at the surface of CeO_2-SnO_2/rGO/GCE are diffusion-controlled rather than surface controlled (Fig. 5b) [28].

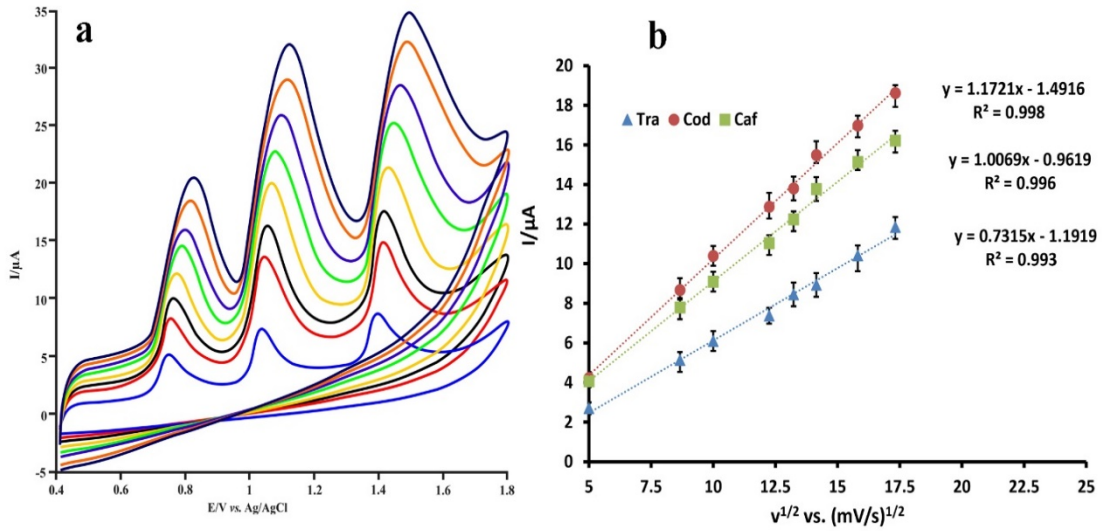

Fig. 5 a) The effect of scan rate on the electrooxidation of Tra, Cod and Caf, b) plot of I *vs.* $v^{1/2}$

In confirmation of the investigation conducted in the previous paragraph, the Semerano coefficient, which can be calculated from the plot slop of Log Ip_a versus Log the scan rate. It can be said that when the Semerano coefficient was about 0.5, the electrochemical process is diffusion-controlled, but it was about 1 the electrochemical surface process is adsorption controlled [28]. So, the changes in logarithm peak currents with variation of logarithm scan rate was plotted for the analytes and the linear regression equations were achieved (Fig. 4c) as Log Ip_a = 0.5864 Log *v* - 0.3906 (R^2 = 0.998), Log Ip_a = 0.5964 Log *v* - 0.1925 (R^2 = 0.996) and Log Ip_a = 0.5617 Log *v* - 0.1693 (R^2 = 0.998) for Tra, Cod, and Caf, respectively. As can be seen, tan α= ΔLog Ip/ΔLog v for Tra, Cod, and Caf were found to be 0.586, 0.596, and 0.5617, close to the theoretical Semerano coefficient of 0.5 so the electrooxidation of three molecules considered to be a diffusion-controlled process.

DPV technique has several parameters, including step potential, modulation potential, scan rate, and equilibrium time which can affect the response of the sensor. These parameters were

investigated and the optimum values were found 0.01 V, 0.025 V, 0.1 V/s, 15 s, respectively and the DPV voltammograms were recorded using the optimized parameters.

3.6. The influence of concentration on response of the electrode

Simultaneous measurement of some drugs can affect the response of the electrode, so by simultaneous and individual determination of target analytes, the effect of them on each other's signal was investigated.

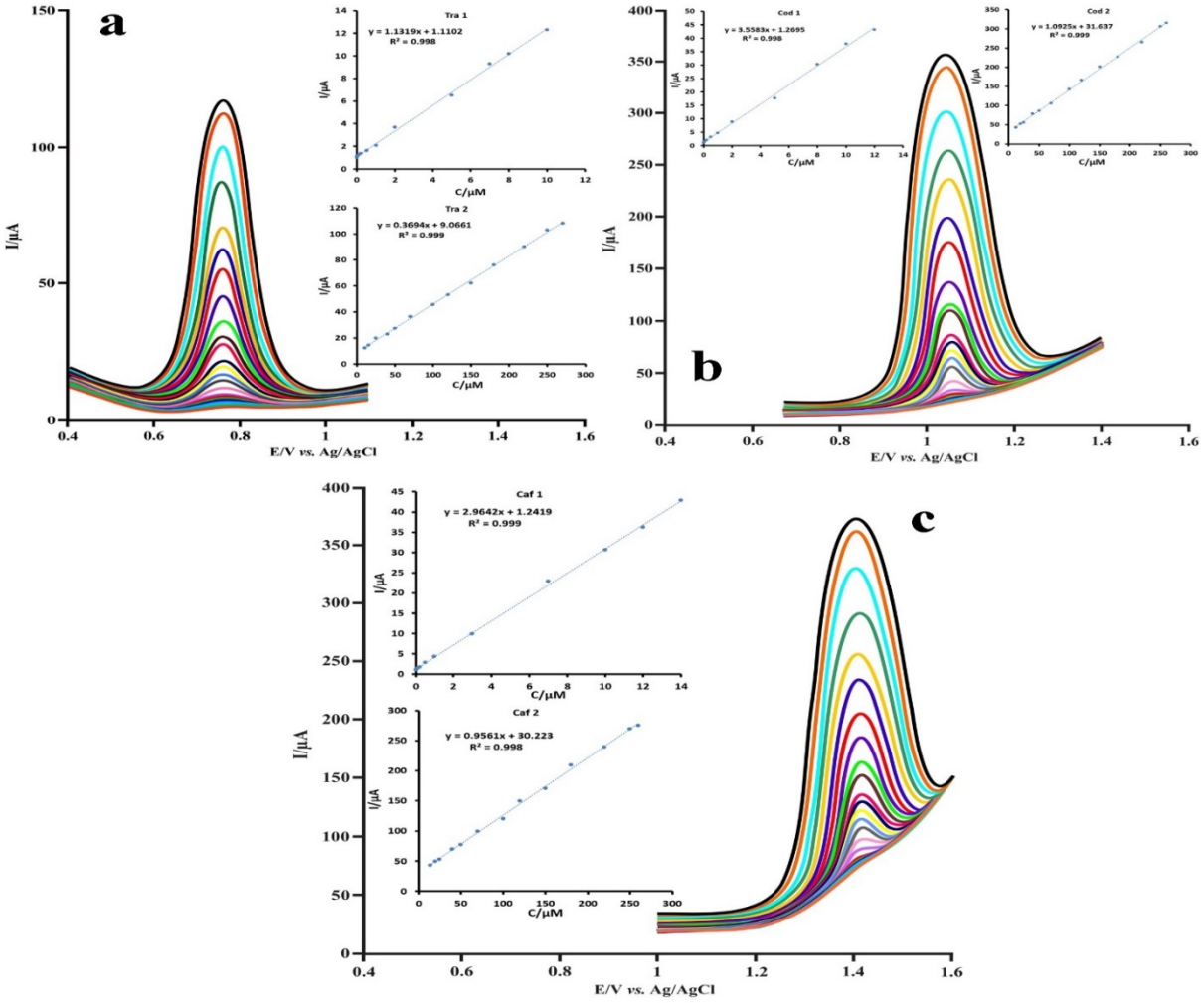

Fig. 6. DPVs of a) Tra, b) Cod and c) Caf at CeO_2-SnO_2/rGO/GCE in B-R buffer solution pH = 6.5

In the first study, the individual determination of Tra, Cod, and Caf by CeO_2-SnO_2/rGO/GCE was done using DPV technique (pH=6.5). The voltammograms are plotted in Fig 6a-c. The voltammetric responses show that two linear dynamic range for each analyte with the calibration equation as follow were obtained.

Tra	0.008-10 µM	Ip = 1.1319 C + 1.1102	R^2 = 0.998	Eq. 4
	10-270 µM	Ip = 0.3694 C + 9.0661	R^2 = 0.999	Eq. 5
Cod	0.01-12 µM	Ip = 3.5583 C + 1.2695	R^2 = 0.998	Eq. 6
	12-260 µM	Ip = 1.0925 C + 31.637	R^2 = 0.999	Eq. 7
Caf	0.01-14 µM	Ip = 2.9642 C + 1.2419	R^2 = 0.999	Eq. 8
	14-260 µM	Ip = 0.9561 C + 30.223	R^2 = 0.998	Eq. 9

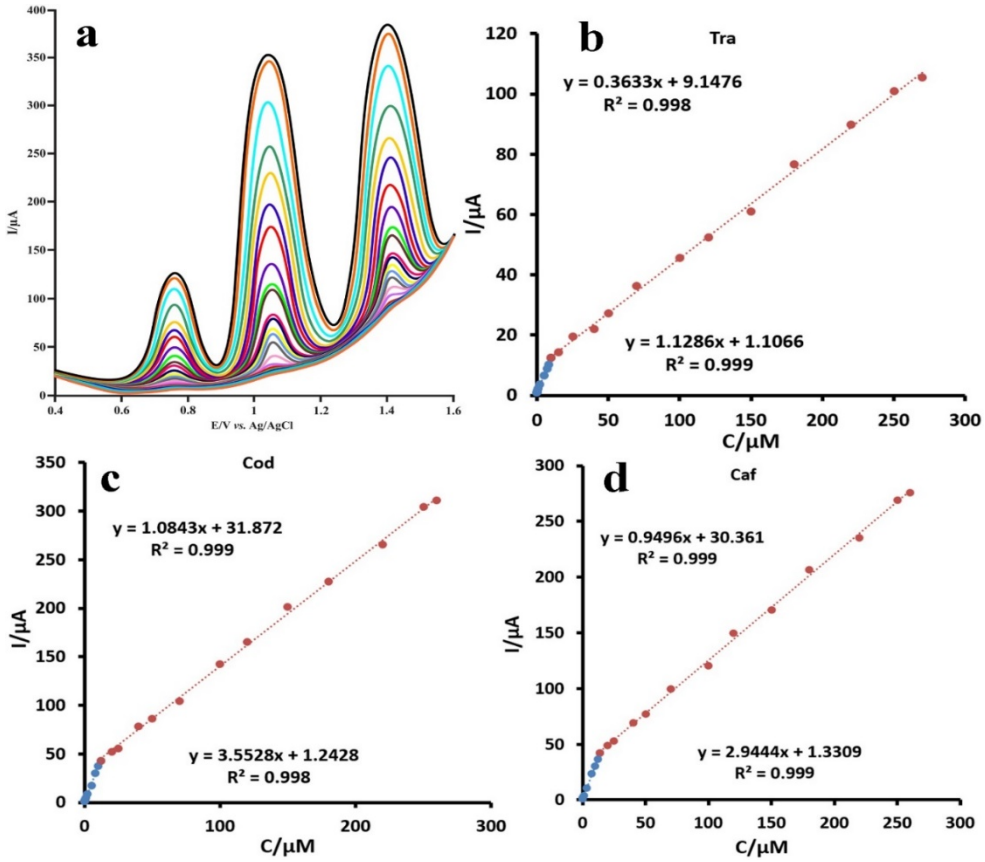

Fig. 7. (a) DPVs at CeO_2-SnO_2/rGO/GCE in optimum condition for simultaneous determination of Tra, Cod and Caf; Calibration plots for (b) Tra, (c) Cod and (d) Caf

In second study, three analytes were determined simultaneously in the optimal condition while the concentration of the three analytes were change with the regression equation of Tra: 0.008-10 (y=1.1286x + 1.1066; R^2 = 0.999) and 10-270 µM (y = 0.3633x + 9.1476: R^2 = 0.998), Cod: 0.01-12 (y = 3.5528x + 1.2428; R^2 = 0.998) and 12-260 µM (y = 1.0843x + 31.872; R^2 = 0.999), Caf: 0.01-14 µM (y = 2.9444x + 1.3309; R^2 = 0.999) and 14-260 µM (y = 0.9496x + 30.361; R^2 = 0.999), the DPV responses are depicted in Fig. 7.

The obtained DLs are computed as three times the standard deviation of the blank over sensitivity (3Sb/m). The DLs for Tra, Cod, and Caf by CeO_2-SnO_2/rGO/GCE were calculated to be 0.0056, 0.0053, and 0.0055 µM, respectively.

Comparing of the currents in individual and simultaneous determination in each concentration for each species shows that there is no significant difference in the DPV current responses. The slopes are almost equal to each other in these two studies, concluding that the three analytes do not have any interference in the measurement of each other.

3.7. Influence of foreign substances

Selectivity of the presented electrode is one of the main parameters that impresses the accuracy of the analysis. Therefore, the selectivity of the presented electrode, and the effect of foreign substances on the voltammetric responses was evaluated by the addition of some ion or molecules which commonly present in the target real samples. The voltammetric responses of the electrode for oxidation of Tra, Cod, and Caf were recorded in the absence and presence of interference species, and the changes in the currents were compared. The tolerance limit was taken as the maximum concentration of the interference species, which lead to a nearly ±5% relative error in voltammetric current.

The tolerated fraction of interference species in the fixed concentration of 0.1 μM Tra, Cod or Caf were investigated. The analysis of the obtained data showed that the oxidation peak current of Tra, Cod or Caf was not affected by even 1100-fold of Li^+, Na^+, K^+, Cl^-, Ca^{2+}, and 200-fold of Uric acid, Ascorbic acid, Morphine, sucrose, and glucose. These results indicate the sufficient selectivity of the presented electrochemical method in the voltammetric measurement of Tra, Cod or Caf.

3.8. Stability, Repeatability, and Reproducibility of the CeO_2-SnO_2/rGO/GCE

The DPVs currents of 10 μM of Tra, Cod or Caf over 10 days were checked the stability of the CeO_2-SnO_2/rGO/GCE. The oxidation peaks current of Tra, Cod or Caf after 10 days was obtained 96%, 96%, and 95%, respectively, in comparison with primary oxidation peak currents. Also, the relative standard deviation (RSD) of oxidation peak currents for Tra, Cod or Caf after 10 days were calculated to be 3.2%, 3.4%, and 3.7%, respectively, which suggested long time stability of electrode responses.

For studying the repeatability of the electrochemical signal of the modified sensor, a solution of 5 μM Tra, Cod or Caf was determined repeatedly for consecutive 10 times. The RSD of determinations were obtained as 2.1%, 1.8%, and 2.4%, respectively, which showed acceptable repeatability for the response of CeO_2-SnO_2/rGO/GCE electrode.

The inter-day reproducibility of CeO_2-SnO_2/rGO/GCE was studied by constructing 7 modified electrodes at different days in a week with a similar fabrication procedure. The RSD value for the peak currents of 5 μM Tra, Cod or Caf with constructed electrodes were obtained as 3.1%, 3.3%, and 3.9%, respectively, which showed admissible reproducibility for the electrochemical response of the sensors.

3.9. Real and spiked sample analysis

The practical application of the presented modified electrode in human urine and blood serum samples was tested by measuring the concentration of Tra, Cod, and Caf to confirm the utility of CeO_2-SnO_2/rGO/GCE. The using real samples were collected from the nearby hospitals.

Table 1. Determination of the analytes in urine and blood serum samples

Sample	Analyte	Added (µM)	Found (µM)	Recovery%	RSD%
Urine	Tra	0	0	-	-
		10	10.34	103.4	1.65
		20	20.86	104.3	2.31
	Cod	0	0	-	-
		10	9.89	98.9	2.24
		20	20.15	100.7	1.98
	Caf	0	0	-	-
		10	9.73	97.3	3.25
		20	19.55	97.8	2.67
Blood serum	Tra	0	0	-	-
		10	10.18	101.8	2.18
		20	19.67	98.4	2.21
	Cod	0	0	-	-
		10	10.31	103.1	3.39
		20	20.14	100.7	2.54
	Caf	0	0	-	-
		10	9.91	99.1	3.01
		20	20.38	101.9	2.96

The standard addition technique was applied to inquire the recovery percentage of Tra, Cod, and Caf in urine and serum samples. Both of samples do not show any response for Tra, Cod, and Caf, informing the absence of the target analytes in the human urine and blood serum. It can be said that, there were three peaks that appeared at -0.02, 0.36, and 0.45 V, which may be related to oxidations of Ascorbic acid, Acetaminophen, and Uric acid, respectively. When 10 and 20 µM of Tra, Cod, and Caf were spiked with the human urine or blood serum, the DPV signals related to Tra, Cod, and Caf were appeared about 0.77, 1.05, and 1.41 V, respectively, and by increasing the concentration the analyte, the current of peaks have increased. The obtained data and the recovery results are tabled in Table 1. The proposed electrochemical method represented recovery percentages between 97.3 and 104.3% for spiked Tra, Cod, and Caf in the human urine and blood serum. In addition, RSD% of all determinations were

calculated and obtain data show that the RSD% were between 1.65, and 3.39%, suggesting that CeO_2-SnO_2/rGO/GCE was reliable, accurate and sensitive and could be applied to measure the target analytes in different human fluids.

Table 2. The comparison of the previous electrochemical methods with the presented method for the determination of Tra, Cod, and Caf

Electrode	Method	Linear range (µM)			Detection limit (µM)			Ref.
		Tra	Cod	Caf	Tra	Cod	Caf	
Poly (Nile blue)/GCE	DPV	1-310	-	0.8-20	0.5	-	0.1	[29]
AuNPs/cysteic acid/GCE	SWV	0.50-63.6	-	-	0.17	-	-	[30]
La^{3+}-CuO/ MWCNT/GCE	DPV	0.5-900	-	-	0.014	-	-	[31]
Nafion/ta-C	DPV	1 – 12.5	-	-	0.131	-	-	[32]
Nafion/GCE	DPV	-	-	63.1–600	-	-	18.9	[33]
GrRAC-70%	DPV	-	-	2.5-1000	-	-	2.94	[34]
TiO2-MCPE	DPV	-	0.7-100	-	-	0.018	-	[35]
SmHCF/MWCNTs / GC	DPAdSV	-	0.2-1 1-20	-	-	0.06	-	[36]
Pt-NiO/ MWCNTs/GCE	DPV	1.0–240	-	-	-	0.084	-	[37]
Boron-doped Diamond Electrode	DPV	3.3-230	-	-	-	0.43	-	[38]
CeO_2-SnO_2/rGO/GCE	DPV	0.008-10 10-270	0.01-12 12-260	0.01-14 14-260	0.0056	0.0053	0.00 55	This work

4. CONCLUSIONS

In this paper, we have represented the simultaneous determination of three important drugs, include Tra, Cod, and Caf, for the first time using CeO_2-SnO_2/rGO modified GCE. The CeO_2-SnO_2/rGO/GCE could shift the oxidation potential of Tra, Cod, and Caf toward less positive potential; however, a small amount, but also boosted their oxidation peak current remarkably when compared to rGO/GCE, SnO_2-rGO/GCE, and bare GCE. At the present electrode, the potential of peaks was separated enough, so individual and simultaneous determination of three analytes could be done. The DPV currents increment linearly while the concentration of Tra, Cod, and Caf have increased and a DLs were found to be 0.0056, 0.0053, and 0.0055 µM, respectively. By comparing the CeO_2-SnO_2/rGO/GCE with previously modified electrodes, it is clear that the presented electrochemical method is comparable and better for the

determination of Tra, Cod, and Caf since it provides the widest linear range and lowest DL (Table 2). Also, the construct of the modified sensor is simple and the reproducibility of the electrode is acceptable. The applicability of the presented method was investigated for the determination of the analytes in urine, and blood serum by the standard addition method. The obtained data demonstrate that the presented electrode can be used in quality control of drug production companies.

REFERENCES

[1] Y. Rostam-Abadi, J. Gholami, M. Amin-Esmaeili, A. Safarcherati, R. Mojtabai, and M.R. Ghadirzadeh, Addiction 115 (2020) 2213.

[2] R. Cairns, A. L. Schaffer, J. A. Brown, S. A. Pearson, and N. A. Buckley, Addiction 115 (2020) 451.

[3] A. G. Engbers, S. Völler, C. F. Poets, C. A. Knibbe, I. K. Reiss, and B. C. Koch, Neonatology 118 (2021) 106.

[4] L. G. Hargis, Analytical chemistry: Principles and techniques (1988).

[5] A. Afkhami, T. Madrakian, S. J. Sabounchei, M. Rezaei, S. Samiee, and M. Pourshahbaz, Sens. Actuators, B 161 (2012) 542.

[6] H. Bagheri, A. Afkhami, H. Khoshsafar, M. Rezaei, and A. Shirzadmehr, Sens. Actuators, B 186 (2013) 451.

[7] H. Bagheri, A. Shirzadmehr, and M. Rezaei, J. Mol. Liq. 212 (2015) 96.

[8] M. Rezaei, Anal. Bioanal. Electrochem., 8 (2016) 287.

[9] H. Khoshsafar, H. Bagheri, M. Rezaei, A. Shirzadmehr, A. Hajian, and Z. Sepehri, J. Electrochem. Soc. 163 (2016) B422.

[10] H. Bagheri, A. Shirzadmehr, and M. Rezaei, Ionics 22 (2016) 1241.

[11] A. Shirzadmehr, M. Rezaei, H. Bagheri, and H. Khoshsafar, Int. J. Environ. Anal. Chem. 96 (2016) 929.

[12] H. Bagheri, A. Shirzadmehr, M. Rezaei, and H. Khoshsafar, Ionics 24 (2018) 833.

[13] S. Zeinali, H. Khoshsafar, M. Rezaei, and H. Bagheri, Anal. Bioanal. Chem. Res., 5 (2018) 195.

[14] N. Pajooheshpour, M. Rezaei, A. Hajian, A. Afkhami, M. Sillanpää, F. Arduini, and H. Bagheri, Sens. Actuators B 275 (2018) 180.

[15] E. Mahmoudi, A. Hajian, M. Rezaei, A. Afkhami, A. Amine, and H. Bagheri, Microchem. J. 145 (2019) 242.

[16] V. Izadkhah, M. Rezaei, and J. Mahmoodi, Anal. Bioanal. Chem. Res. 6 (2019) 405.

[17] M. Coros, F. Pogacean, A. Turza, M. Dan, C. Berghian-Grosan, I. O. Pana, and S. Pruneanu, Phys. E, 119 (2020) 113971.

[18] A. Umar, T. Almas, A. A. Ibrahim, R. Kumar, M. AlAssiri, S. Baskoutas, and M. S. Akhtar, J. Electroanal. Chem., 864 (2020) 114089.

[19] S. Matussin, M. H. Harunsani, A.L. Tan, and M. M. Khan, ACS Sustainable Chem. Eng. 8 (2020) 3040.
[20] J. T. Robinson, F. K. Perkins, E. S. Snow, Z. Wei, and P. E. Sheehan, Nano Lett. 8 (2008) 3137.
[21] N. Mohammadi, and M. Bahmaei, A. Anal. Bioanal. Electrochem. 12 (2020) 468.
[22] A. Priyadharsan, V. Vasanthakumar, S. Karthikeyan, V. Raj, S. Shanavas, and P. Anbarasan, J. Photochem. Photobiol. A 346 (2017) 32.
[23] F. Tadayon, and M. N. Jahromi, J. Iran. Chem. Soc. 17 (2020) 847.
[24] T. M. Al-Saadi, B. H. Hussein, A. B. Hasan, and A. Shehab, Energy Procedia 157 (2019) 457.
[25] X. Lv, G. Liang, Y. Li, H. Duan, D. Chen, and M. Long, Properties and Microstructure of Copper and/or Nickel Supported on GO, rGO, and NGO, Energy Technology 2020: Recycling, Carbon Dioxide Management, and Other Technologies, Springer (2020) pp. 127-135.
[26] J. M. P. J. Garrido, C. Delerue-Matos, F. Borges, T. R. Macedo, and A. Oliveira-Brett, Electroanalysis, 16 (2004) 1427-33.
[27] A. A. Ensafi, E. Heydari-Bafrooei, and B. Rezaei, Biosens. Bioelectron. 41 (2013) 627.
[28] H. Zeinali, H. Bagheri, Z. Monsef-Khoshhesab, H. Khoshsafar, and A. Hajian, Mater. Sci. Eng. C 71 (2017) 386.
[29] S. Chitravathi, and N. Munichandraiah, J. Electroanal. Chem. 764 (2016) 93.
[30] Z. Hassanvand, and F. Jalali, Anal. Bioanal. Chem. Res. 6 (2019) 393.
[31] M. M. Foroughi, S. Jahani, and H. H. Nadiki, Sens. Actuators B 285 (2019) 562.
[32] E. Mynttinen, N. Wester, T. Lilius, E. Kalso, J. Koskinen, and T. Laurila, Electrochim. Acta 295 (2019) 347.
[33] A. S. Farag, K. Pravcová, L. Česlová, K. Vytřas, and M. Sýs, Electroanalysis 31 (2019) 1494.
[34] M. K. Monteiro, S. S. Paiva, D. R. da Silva, V. J. Vilar, C. A. Martínez-Huitle, and E. V. dos Santos, J. Electroanal. Chem. 839 (2019) 283.
[35] M. H. Mashhadizadeh, and F. Rasouli, Electroanalysis 26 (2014) 2033.
[36] M. H. Mashadizadeh, G. Abdollahi, and T. Yousefi, J. Electroanal. Chem. 780 (2016) 68.
[37] A. Dehdashti, and A. Babaei, J. Electroanal. Chem. 862 (2020) 113949.
[38] O. Yunusoğlu, S. Allahverdiyeva, Y. Yardım, and Z. Şentürk, Electroanalysis 32 (2020) 429.